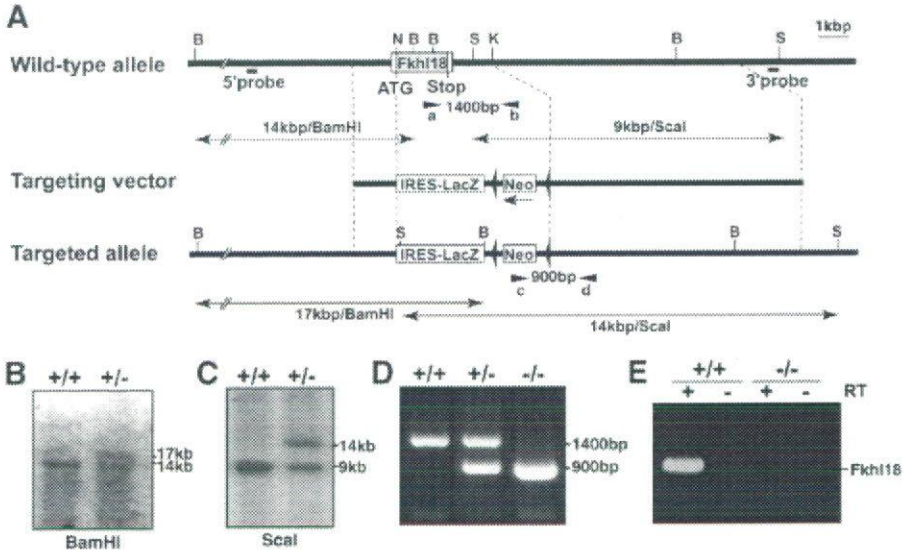


**Fig. 3.** Generation of *Fkhl18* KO mice. **A**: Generation of targeted allele of *Fkhl18*. Wild-type (WT) *Fkhl18* locus (top), targeting vector (middle), and targeted locus (bottom) are shown. *Fkhl18* gene consists of a single exon. Shaded and open boxes indicate coding and noncoding regions, respectively. The *Nco*I/*Kpn*I fragment of *Fkhl18* gene encoding 29th to 329th amino acid residues was replaced by IRES-lacZ-pMC1neo cassette in the targeting vector. Homologous recombination between the WT and targeting vector is expected to generate the targeted allele lacking the *Nco*I/*Kpn*I fragment. B; *Bam*HI, S; *Sca*I, N; *Nco*I. K; *Kpn*I. **B**: Southern blotting of *Bam*HI digested tail DNA from WT (+/+) and heterozygous (+/−) for *Fkhl18* KO. After the *Bam*HI digested DNAs were separated by agarose gel electrophoresis, the DNAs transferred to membrane were hybridized with the 5′ probe indicated in (A). The 5′ probe detected a 14-kb fragment in the WT mouse, and both 14-kb and 17-kb fragments in the heterozygous mouse. **C**: Southern blotting of *Sca*I digested tail DNA from WT (+/+) and heterozygous (+/−) for *Fkhl18* KO. The DNAs were hybridized with the 3′ probe is indicated in (A). The 3′ probes detected a 9 kb fragment in the WT mouse, and both 9 and 14 kb fragments in the heterozygous mouse. **D**: Genomic PCR to distinguish homozygous, heterozygous, and WT for *Fkhl18* KO. Genomic DNAs were extracted from tails of the fetuses and subjected to PCR analyses using primers a and b, and c and d. PCR product of 1.4 kb length is detected in the WT (+/+), both 1.4 and 0.9 kb are detected in the heterozygous (+/−), and 0.9 kb is detected in homozygous (−/−) fetuses. **E**: RT-PCR analyses of *Fkhl18* expression. Total RNAs were prepared from E14.5 fetal testes of the WT (+/+) and homozygous (−/−) KO, and were analyzed by RT-PCR.

dark and blurred in the *Fkhl18* KO testes. Thus, the gonads were sectioned, and we found leaking of the injected carbon ink from the testicular vessels (Fig. 4C-c,d) and coelomic vessel (Fig. 4C-e,f). The leakage of the carbon ink suggested a defect in the sealing structure of the vasculature in the *Fkhl18* KO mice. Further examination of the fine structure of the testicular vasculature by electron microscopy showed the presence of hole in the endothelial cells of the *Fkhl18* KO testes; the holes varied in size from 100 to 400 nm were devoid of any membrane and allowed extravasation of carbon ink (Fig. 4D). Usually, one gap was noticed in every 10 cross sections of capillaries. Obvious defect was not observed in the periendothelial cells. Any abnormality was never seen in the vasculature of WT.

### Apoptosis of Periendothelial Cells in Fkhl18 KO Fetal Testis

The above structural defect suggested ectopic apoptosis of cells in the vasculature system of the *Fkhl18* KO testis. To test this, we examined the expression of caspase 3 in the WT and KO testes. As expected, caspase 3-positive cells (green in Fig. 5A) were found adjacent to vascular endothelial cells (red in Fig. 5A) in the KO testes. Considering the spatial correlation between caspase 3-positive cells and PECAM1-positive endothelial cells, we concluded that the apoptotic cells were periendothelial cells. To confirm this, we used *Fkhl18* KO mouse harboring #51 Tg construct (Fkhl18KO; Fkhl18-lacZ Tg). As shown in Figure 5B, caspase 3-positive signals overlapped with lacZ staining. The density of apoptotic cells in the KO testes was approximately threefold that in the WT (n = 4 fetuses each; Fig. 5C). These findings suggest that apoptosis of periendothelial cells in the absence of *Fkhl18* leads to defective testicular vascular system.

### Possible Involvement of Fkhl18 in Regulation of Fas Ligand Gene Expression

Fox proteins share a winged helix DNA-binding domain and are known to act as transcription factors. To investigate whether Fkhl18 have a transcriptional activity, we performed reporter gene assays using p6 × DBE-luc containing six repeats of Fox consensus sequence. As described previously (Furuyama et al., 2000), both FoxO3a and FoxO4 activated the transcription of p6 × DBE-luc, whereas *Fkhl18* did not show any activity by itself (Fig. 6A). Therefore, we examined whether *Fkhl18* acts as a suppressor against FoxO3a and FoxO4. When Fkhl18 was co-expressed with FoxO3a or FoxO4, the activities driven by FoxO3a and FoxO4 were suppressed in a dose-dependent manner (Fig. 6A).

Next, we examined the DNA binding activity of Fkhl18 by EMSA (Fig. 6B). In vitro synthesized myc-tagged Fkhl18 bound to Fox consensus sequence (WT)

but not to mutated sequence (mut), and this binding signal disappeared in a dose-dependent manner following the addition of nonlabeled WT oligonucleotides. The results of the in vitro EMSA study suggest that the transcriptional suppression by Fkhl18 is due to competitive binding between Fkhl18 and FoxOs, although it was unknown whether Fkhl18 is localized in the nucleus or not. To check this, we examined intracellular distribution of myc-tagged Fkhl18 (Fkhl18-myc) in cultured cells. As shown in Figure 6C, FoxO3 and FoxO4 were localized exclusively in the nucleus, while Fkhl18 was localized predominantly in the nucleus. Together with the results of the reporter gene assays, it is likely that Fkhl18 suppresses the activities of other Fox proteins possibly through competitively occupying the target site on gene promoters.

As described above, our study showed that disruption of *Fkhl18* resulted in ectopic apoptosis of periendothelial cells. Considering the suppressive function of Fkhl18, we assumed that genes necessary for the occurrence of apoptosis would be suppressed in WT. Consistent with this assumption, it was reported that *FasL* gene expression is activated by Fox proteins (Brunet et al., 1999). Therefore, we investigated whether Fkhl18 suppresses human and mouse *FasL* promoter activities. As we expected, Fkhl18 suppressed, dose-dependently, human and mouse *FasL* promoter in bovine vascular smooth muscle cells (Fig. 6D). Considered together, these results suggest that Fkhl18 potentially suppresses proapoptotic signals by associating the Fox consensus element in *FasL* promoter.

## DISCUSSION

Development of the vascular system of animals starts at fetal age. Primitive vasculature consisting of small capillaries develops from blood vessel precursor cells, and the primitive vessels expand progressively, producing branches to form the vascular tree. At the early stage of blood vessel formation (angiogenesis and arteriogenesis), periendothelial cells as well as endothelial cells are required for generation of a functional vascular system (Carmeliet, 2003, 2005). The requirement of endothelial and periendothelial cells is strongly suggestive of a functional correlation between the two cell types during blood vessel development. In the present study, we demonstrated the expression of *Fkhl18* in periendothelial cells encircling the endothelial cells in the

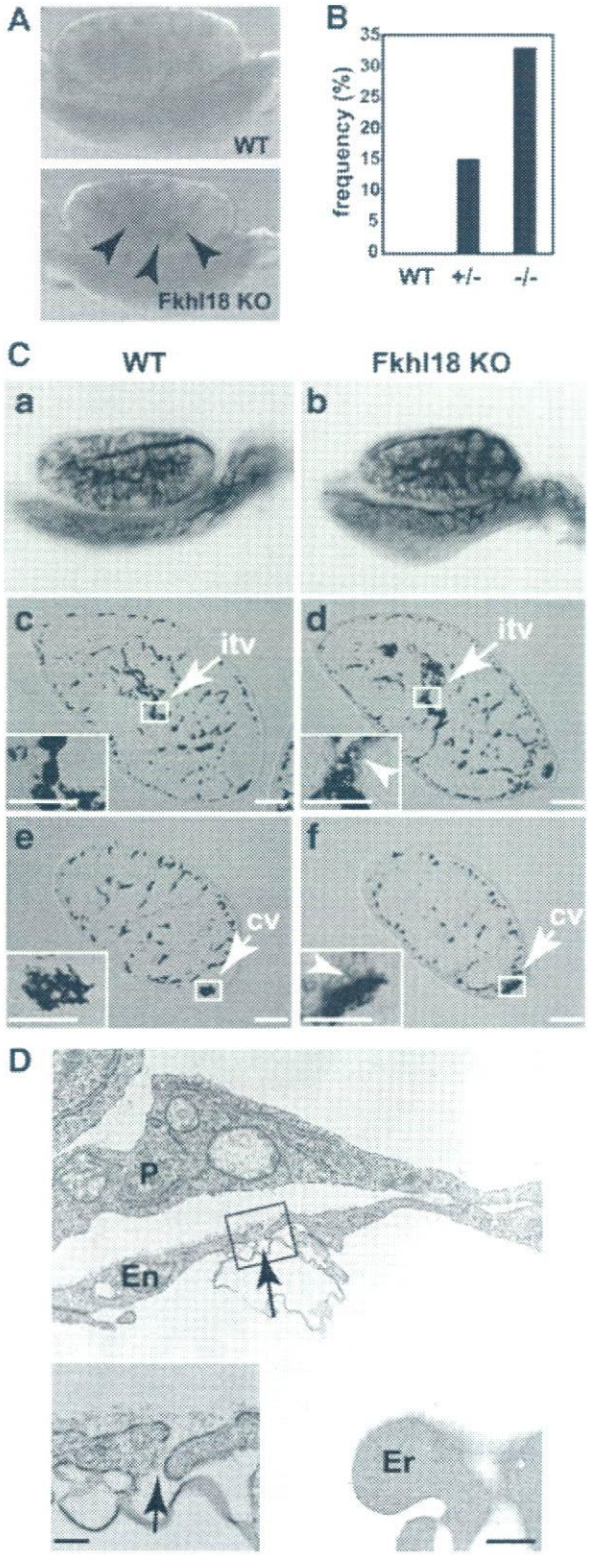


**Fig. 4.** Testicular vasculature abnormalities in *Fkhl18* KO mice. **A**: Appearance of dissected fetal testes of WT and *Fkhl18* KO. Note the accumulation of blood cells in the central part of the *Fkhl18* KO testis (arrowheads). **B**: Frequency of blood accumulation examined in 14 WT, 26 heterozygous (+/−) and 12 homozygous (−/−) testes. Frequency (%) of testes showing blood accumulation relative to total number of testes examined are shown. **C**: Visualization of the vasculature structure using carbon ink. Carbon ink was injected into the testes through the umbilical vein. The whole views of the WT (a) and *Fkhl18* KO testes (b) are shown. The WT (c, e) and *Fkhl18* KO (d, f) testes were sectioned. Areas containing inner testicular vessels (itv; c, d) and coelomic vessels (cv; e, f) are enlarged in insets. As indicated by arrowheads in insets of (d) and (f), leakage of the injected ink was noted around the vessels of *Fkhl18* KO testes. Scale bars = 100 μm, scale bars in insets = 50 μm. **D**: Electron microscopic view of a representative *Fkhl18* KO testis. The area enclosed by the rectangle is enlarged as the inset. Arrows indicate a gap in endothelial cells in KO testis. En; endothelial cell, P; periendothelial cell, Er; erythrocyte. Scale bars = 500 μm, scale bars in insets = 100 μm.

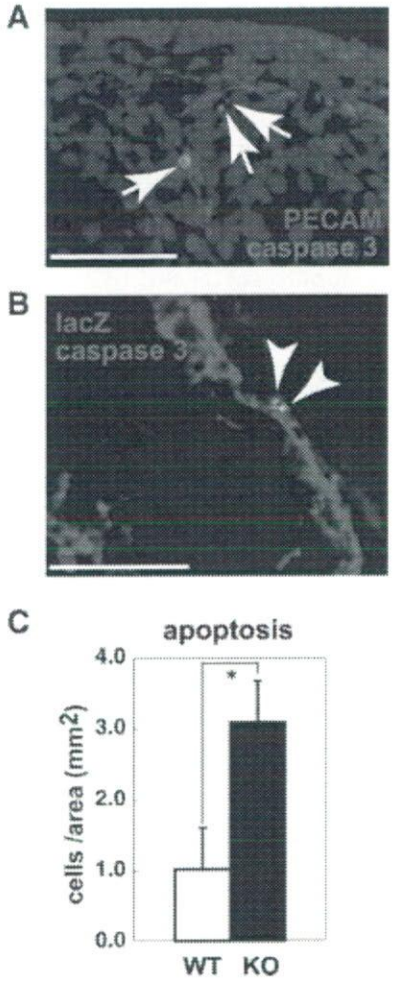


**Fig. 5.** Marked apoptosis of periendothelial cells in *Fkhl18* KO testis. **A**: Expression of caspase 3 in the *Fkhl18* KO fetal testis. *Fkhl18* KO E14.5 testis was immunostained with caspase 3 antibody (green) and PECAM (red). As indicated by arrows, caspase 3-positive cells are localized adjacent to PECAM-positive endothelial cells (red). Nuclei were counterstained with DAPI (blue). Scale bars = 50 μm. **B**: Expression of caspase 3 in periendothelial cells of the *Fkhl18* KO fetal testis. Double immunostaining for lacZ and caspase 3 was performed in E14.5 testes of Fkhl18KO; Fkhl18-lacZ Tg mice. As indicated by arrowheads, caspase 3-positive cells (green) overlapped with Fkhl18-positive cells (red). Scale bars = 50 μm. **C**: Apoptosis of vascular periendothelial cells. Caspase 3-positive cells adjacent to endothelial cells were counted in WT and *Fkhl18* KO fetal testes. Data are mean ± SD numbers of caspase 3-positive cells per unit area ($mm^2$). $^*P < 0.02$.

developing fetal testis. *Fkhl18*-deficient mice displayed the following testicular abnormalities during fetal life; (1) accumulation of blood cells in the central part of the fetal testis, (2) presence of gaps, measuring 100–400 nm in diameter, in endothelial cells, allowing leakage of injected carbon ink from the testicular vessels, and (3) aberrant apoptosis of periendothelial cells. These features strongly suggest the importance of *Fkhl18* expression in the periendothelial cells for development of the testicular vascular system through direct and indirect regulation of the functions of periendothelial and endothelial cells, respectively.

This indirect function of *Fkhl18* indicates a functional interaction between endothelial and periendothelial cells. The importance of interactions between the two cell types for vascular maturation has been examined by gene knockout studies. For example, angiopoietin-1 is expressed in periendothelial cells, while its receptor *TIE-2* is expressed in endothelial cells. In the absence of periendothelial angiopoietin-1, endothelial cells do not properly recruit and associate with periendothelial supporting cells (Suri et al., 1996). This ligand/receptor interaction represents a signaling pathway from periendothelial to endothelial cells. As a reciprocal signaling pathway, functional correlation between platelet-derived growth factor (PDGF)-BB expressed in endothelial cells and PDGF receptor β (PDGFRβ) in periendothelial cells was demonstrated (Hellstrom et al., 1999). Recruitment of periendothelial cells expressing *PDGFRβ* was affected when *PDGF-BB* gene was disrupted. Unlike the KO mice described above, recruitment of periendothelial cells did not seem to be affected in the fetal testes of *Fkhl18* KO mice. Interestingly, however, marked apoptosis of periendothelial cells was observed; with resultant focal and transient loss of periendothelial cells. Since *Fkhl18* is not expressed in endothelial cells, the structural defect induced in endothelial cells possibly resulted from weakened interaction with the affected or decreased periendothelial cells.

Male-specific patterning of the vasculature in the developing testis is induced by *Sry* (Buehr et al., 1993; Martineau et al., 1997; Capel et al., 1999; Tilmann and Capel, 1999; Brennan et al., 2002, 2003). Following the expression of *Sry*, endothelial cells are recruited vigorously to the testis from mesonephros to develop the male specific coelomic vessel. Thereafter, the vessel branches from the coelomic vessel and extends progressively between testicular cords. Although blood vessels are also formed in the ovary, such active event of blood vessel formation never occurs in the ovary at the fetal stage. In this study, we noticed blood cell accumulation in the central part of the fetal testis in most *Fkhl18* KO fetuses. However, such defect was never seen in the female KO ovary (data not shown). This sexually dimorphic defect seems to correlate with the differential development of blood vessels in the two sexes. Moreover, the expression of *Fkhl18* in the testis is significantly higher than in the ovary. Taken together, higher amount of *Fkhl18* would be required for the active organization of the vasculature system.

Reporter gene assays revealed that Fkhl18 suppresses transcription mediated by *FoxO3a* and *FoxO4*. Since Fkhl18 can bind to consensus DNA binding sequence for *Fox*, it potentially represses transcription by competing for binding sites with other Fox proteins. Considering the suppressive function of Fkhl18, it is interesting to note that FoxOs mediate proapoptotic gene expression. For example, overexpression of FoxOs resulted in apoptosis through direct induction of tumor-necrosis factor-related apoptosis-inducing ligand (TRAIL) in prostate cancer (Modur et al., 2002). In neurons deprived of nerve growth factor (NGF), FoxO3a

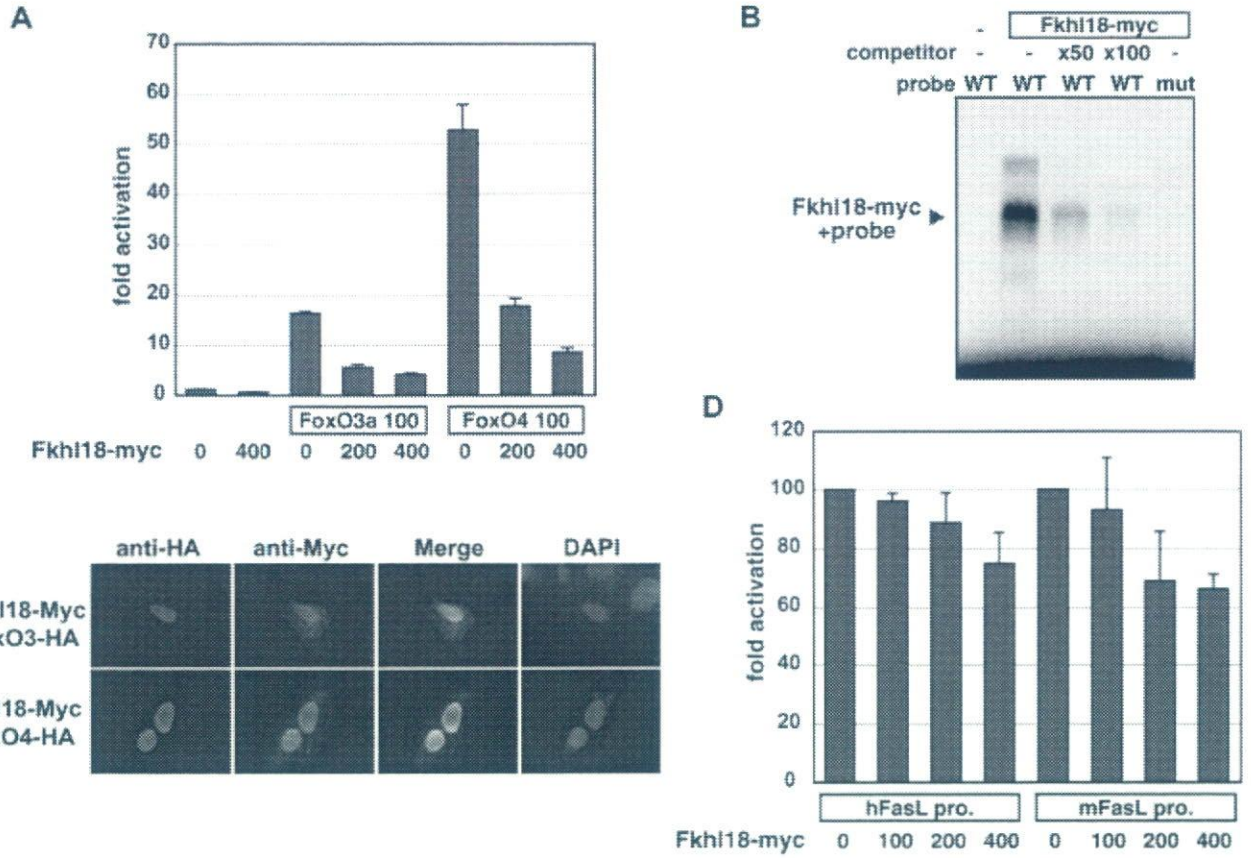


**Fig. 6.** Possible transcriptional suppression of Fas ligand gene by Fkhl18. **A**: Transcriptional suppression by Fkhl18. Expression vectors for Fkhl18 (400 ng) or FoxO3a (100 ng), FoxO4 (100 ng) were transfected into U2OS cells with p6 × DBE-luc reporter gene containing six repeats of consensus binding sequence for forkhead proteins (200 ng), and β-galactosidase (25 ng). For effects of Fkhl18 on FoxOs' activity, increasing amounts of Fkhl18 (200, 400 ng) were transfected with FoxO3a (100 ng) or FoxO4 (100 ng). Results are mean ± SD of triplicate transfections. Data represent the ratio of luciferase activity normalized by β-galactosidase activity to basal reporter activity. **B**: EMSAs performed with WT and mutated Fox consensus sequences. In vitro synthesized Fkhl18-myc was incubated with WT and mutated oligonucleotides (mut). Fifty or 100-fold excess amount of unlabeled oligonucleotide (WT) was used as a competitor. Arrowhead indicates retarded signal. **C**: Intracellular localization of Fkhl18. Fkhl18-myc (green), FoxO3-HA (HA-tagged FoxO3), and FoxO4-HA (HA-tagged FoxO4) were transfected into U2OS cells and their intracellular distribution was examined. Cells were counterstained with DAPI (blue). **D**: Suppressive effect of Fkhl18 on FasL promoter. Increasing amount of Fkhl18 expression vector (100, 200, 400 ng) were transfected into bovine vascular smooth muscle cells with human or mouse FasLpro-luc reporter gene (200 ng), and β-galactosidase (20 ng). Results are mean ± SD of three independent experiments. Data represent the ratio of luciferase activity normalized by β-galactosidase activity to basal reporter activity.

directly activated *bim* (Bcl-2 interacting mediator of cell death) promoter via conserved Fox binding sites (Gilley et al., 2003). Moreover, *Akt* activated by survival factors phosphorylated *FoxO3a* and thereby prevented the association of *FoxO3a* to *FasL* promoter (Brunet et al., 1999). Based on the results published so far, we hypothesized that the marked apoptosis of periendothelial cells in *Fkhl18* KO testes is caused by defective proapoptotic gene transcription, which is normally attenuated by Fkhl18. As expected, Fkhl18 suppressed transcription from *FasL* gene promoter in cultured smooth muscle cells prepared form bovine blood vessels, although such suppression seemed inefficient. We assumed that the inefficient suppression was due to cellular condition since normally *FasL* gene expression should be activated by apoptotic signal. Therefore, we carried out the reporter gene assays using cells treated with okadaic acid, which is known to activate the apoptotic process (Rossini et al., 1997; Goto et al., 2002; Fujita et al., 2004). Unfortunately, however, the reporter gene was probably abnormally transcribed, most likely because of the toxicity of okadaic acid (Rossini et al., 1997). Therefore, although the reason for the ineffective suppression by Fkhl18 remains to be clarified, it is possible that Fkhl18 modulates transcription driven by other Fox transcription factors in periendothelial cells.

In the present study, we focused on the function of *Fkhl18* during blood vessel formation of the fetal testis; blood vessel development in the ovary remains to be investigated. Likewise, we have not examined whether the blood vessels in tissues other than the gonads are affected by *Fkhl18*. Considering that *Fkhl18* is expressed in periendothelial cells of other tissues, the defects seen in the fetal testis could be also seen in other tissues. However, obvious accumulation of blood cells was not observed in any tissues other than the testis, strongly arguing against a major defect of blood vessel

development in these tissues. Together with the highest expression of *Fkhl18* in the developing testis, it is conceivable that *Fkhl18* plays a unique role in the development of the testicular vasculature system.

## ACKNOWLEDGMENTS

We thank Dr. K. Mihara and Dr. M. Sakaguchi (Kyushu University) for providing antiserum to lacZ. This work was supported in part by Grants-in-Aid for Scientific Research (S) and Grants-in-Aid for Scientific Research on Priority Areas from the Ministry of Education, Culture, Sports Science, and Technology of Japan, and Japan Science and Technology Corporation.

## REFERENCES

Accili D, Arden KC. 2004. FoxOs at the crossroads of cellular metabolism, differentiation, and transformation. Cell 117:421–426.

Ang SL, Rossant J. 1994. HNF-3 beta is essential for node and notochord formation in mouse development. Cell 78:561–574.

Aoyama T, Chen M, Fujiwara H, Masaki T, Sawamura T. 2000. LOX-1 mediates lysophosphatidylcholine-induced oxidized LDL uptake in smooth muscle cells. FEBS Lett 467:217–220.

Brennan J, Capel B. 2004. One tissue, two fates: Molecular genetic events that underlie testis versus ovary development. Nat Rev Genet 5:509–521.

Brennan J, Karl J, Capel B. 2002. Divergent vascular mechanisms downstream of Sry establish the arterial system in the XY gonad. Dev Biol 244:418–428.

Brennan J, Tilmann C, Capel B. 2003. Pdgfr-alpha mediates testis cord organization and fetal Leydig cell development in the XY gonad. Genes Dev 17:800–810.

Brice G, Mansour S, Bell R, Collin JR, Child AH, Brady AF, Sarfarazi M, Burnand KG, Jeffery S, Mortimer P, Murday VA. 2002. Analysis of the phenotypic abnormalities in lymphoedema-distichiasis syndrome in 74 patients with FOXC2 mutations or linkage to 16q24. J Med Genet 39:478–483.

Brunet A, Bonni A, Zigmond MJ, Lin MZ, Juo P, Hu LS, Anderson MJ, Arden KC, Blenis J, Greenberg ME. 1999. Akt promotes cell survival by phosphorylating and inhibiting a Forkhead transcription factor. Cell 96:857–868.

Buehr M, Gu S, McLaren A. 1993. Mesonephric contribution to testis differentiation in the fetal mouse. Development 117:273–281.

Capel B, Albrecht KH, Washburn LL, Eicher EM. 1999. Migration of mesonephric cells into the mammalian gonad depends on Sry. Mech Dev 84:127–131.

Carmeliet P. 2003. Angiogenesis in health and disease. Nat Med 9:653–660.

Carmeliet P. 2005. Angiogenesis in life, disease and medicine. Nature 438:932–936.

Castanet M, Park SM, Smith A, Bost M, Leger J, Lyonnet S, Pelet A, Czernichow P, Chatterjee K, Polak M. 2002. A novel loss-of-function mutation in TTF-2 is associated with congenital hypothyroidism, thyroid agenesis and cleft palate. Hum Mol Genet 11:2051–2059.

Chatila TA, Blaeser F, Ho N, Lederman HM, Voulgaropoulos C, Helms C, Bowcock AM. 2000. JM2, encoding a fork head-related protein, is mutated in X-linked autoimmunity-allergic disregulation syndrome. J Clin Invest 106:R75–R81.

Chen X, Rubock MJ, Whitman M. 1996. A transcriptional partner for MAD proteins in TGF-beta signalling. Nature 383:691–696.

Chen X, Weisberg E, Fridmacher V, Watanabe M, Naco G, Whitman M. 1997. Smad4 and FAST-1 in the assembly of activin-responsive factor. Nature 389:85–89.

Crisponi L, Deiana M, Loi A, Chiappe F, Uda M, Amati P, Bisceglia L, Zelante L, Nagaraja R, Porcu S, Ristaldi MS, Marzella R, Rocchi M, Nicolino M, Lienhardt-Roussie A, Nivelon A, Verloes A, Schlessinger D, Gasparini P, Bonneau D, Cao A, Pilia G. 2001. The putative forkhead transcription factor FOXL2 is mutated in blepharophimosis/ptosis/epicanthus inversus syndrome. Nat Genet 27:159–166.

Erickson RP, Dagenais SL, Caulder MS, Downs CA, Herman G, Jones MC, Kerstjens-Frederikse WS, Lidral AC, McDonald M, Nelson CC, Witte M, Glover TW. 2001. Clinical heterogeneity in lymphoedema-distichiasis with FOXC2 truncating mutations. J Med Genet 38:761–766.

Frank J, Pignata C, Panteleyev AA, Prowse DM, Baden H, Weiner L, Gaetaniello L, Ahmad W, Pozzi N, Cserhalmi-Friedman PB, Aita VM, Uyttendaele H, Gordon D, Ott J, Brissette JL, Christiano AM. 1999. Exposing the human nude phenotype. Nature 398:473–474.

Fujita M, Goto K, Yoshida K, Okamura H, Morimoto H, Kito S, Fukuda J, Haneji T. 2004. Okadaic acid stimulates expression of Fas receptor and Fas ligand by activation of nuclear factor kappa-B in human oral squamous carcinoma cells. Oral Oncol 40:199–206.

Furuyama T, Nakazawa T, Nakano I, Mori N. 2000. Identification of the differential distribution patterns of mRNAs and consensus binding sequences for mouse DAF-16 homologues. Biochem J 349:629–634.

Galili N, Davis RJ, Fredericks WJ, Mukhopadhyay S, Rauscher FJ III, Emanuel BS, Rovera G, Barr FG. 1993. Fusion of a fork head domain gene to PAX3 in the solid tumour alveolar rhabdomyosarcoma. Nat Genet 5:230–235.

Gilley J, Coffer PJ, Ham J. 2003. FOXO transcription factors directly activate bim gene expression and promote apoptosis in sympathetic neurons. J Cell Biol 162:613–622.

Goto K, Fukuda J, Haneji T. 2002. Okadaic acid stimulates apoptosis through expression of Fas receptor and Fas ligand in human oral squamous carcinoma cells. Oral Oncol 38:16–22.

Harris SE, Chand AL, Winship IM, Gersak K, Aittomaki K, Shelling AN. 2002. Identification of novel mutations in FOXL2 associated with premature ovarian failure. Mol Hum Reprod 8:729–733.

Hellstrom M, Kalen M, Lindahl P, Abramsson A, Betsholtz C. 1999. Role of PDGF-B and PDGFR-beta in recruitment of vascular smooth muscle cells and pericytes during embryonic blood vessel formation in the mouse. Development 126:3047–3055.

Hillion J, Le Coniat M, Jonveaux P, Berger R, Bernard OA. 1997. AF6q21, a novel partner of the MLL gene in t(6;11)(q21;q23), defines a forkhead transcriptional factor subfamily. Blood 90:3714–3719.

Hulander M, Wurst W, Carlsson P, Enerback S. 1998. The winged helix transcription factor Fkh10 is required for normal development of the inner ear. Nat Genet 20:374–376.

Hulander M, Kiernan AE, Blomqvist SR, Carlsson P, Samuelsson EJ, Johansson BR, Steel KP, Enerback S. 2003. Lack of pendrin expression leads to deafness and expansion of the endolymphatic compartment in inner ears of Foxi1 null mutant mice. Development 130:2013–2025.

Kaestner KH, Lee KH, Schlondorff J, Hiemisch H, Monaghan AP, Schutz G. 1993. Six members of the mouse forkhead gene family are developmentally regulated. Proc Natl Acad Sci USA 90:7628–7631.

Katoh-Fukui Y, Tsuchiya R, Shiroishi T, Nakahara Y, Hashimoto N, Noguchi K, Higashinakagawa T. 1998. Male-to-female sex reversal in M33 mutant mice. Nature 393:688–692.

Katoh-Fukui Y, Owaki A, Toyama Y, Kusaka M, Shinohara Y, Maekawa M, Toshimori K, Morohashi K. 2005. Mouse Polycomb M33 is required for splenic vascular and adrenal gland formation through regulating Ad4BP/SF1 expression. Blood 106:1612–1620.

Kitamura K, Yanazawa M, Sugiyama N, Miura H, Iizuka-Kogo A, Kusaka M, Omichi K, Suzuki R, Kato-Fukui Y, Kamiirisa K, Matsuo M, Kamijo S, Kasahara M, Yoshioka H, Ogata T, Fukuda T, Kondo I, Kato M, Dobyns WB, Yokoyama M, Morohashi K. 2002. Mutation of ARX causes abnormal development of forebrain and testes in mice and X-linked lissencephaly with abnormal genitalia in humans. Nat Genet 32:359–369.

Koopman P, Munsterberg A, Capel B, Vivian N, Lovell-Badge R. 1990. Expression of a candidate sex-determining gene during mouse testis differentiation. Nature 348:450–452.

Labosky PA, Winnier GE, Jetton TL, Hargett L, Ryan AK, Rosenfeld MG, Parlow AF, Hogan BL. 1997. The winged helix gene, Mf3, is required for normal development of the diencephalon and midbrain, postnatal growth and the milk-ejection reflex. Development 124: 1263–1274.

Lai CS, Fisher SE, Hurst JA, Vargha-Khadem F, Monaco AP. 2001. A forkhead-domain gene is mutated in a severe speech and language disorder. Nature 413:519–523.

Lin L, Miller CT, Contreras JI, Prescott MS, Dagenais SL, Wu R, Yee J, Orringer MB, Misek DE, Hanash SM, Glover TW, Beer DG. 2002. The hepatocyte nuclear factor 3 alpha gene, HNF3alpha (FOXA1), on chromosome band 14q13 is amplified and overexpressed in esophageal and lung adenocarcinomas. Cancer Res 62:5273–5279.

Martineau J, Nordqvist K, Tilmann C, Lovell-Badge R, Capel B. 1997. Male-specific cell migration into the developing gonad. Curr Biol 7:958–968.

Mears AJ, Jordan T, Mirzayans F, Dubois S, Kume T, Parlee M, Ritch R, Koop B, Kuo WL, Collins C, Marshall J, Gould DB, Pearce W, Carlsson P, Enerback S, Morissette J, Bhattacharya S, Hogan B, Raymond V, Walter MA. 1998. Mutations of the forkhead/winged-helix gene, FKHL7, in patients with Axenfeld-Rieger anomaly. Am J Hum Genet 63:1316–1328.

Modur V, Nagarajan R, Evers BM, Milbrandt J. 2002. FOXO proteins regulate tumor necrosis factor-related apoptosis inducing ligand expression. Implications for PTEN mutation in prostate cancer. J Biol Chem 277:47928–47937.

Morohashi K, Honda S, Inomata Y, Handa H, Omura T. 1992. A common trans-acting factor, Ad4-binding protein, to the promoters of steroidogenic P-450s. J Biol Chem 267:17913–17919.

Morohashi K, Iida H, Nomura M, Hatano O, Honda S, Tsukiyama T, Niwa O, Hara T, Takakusu A, Shibata Y., et al. 1994. Functional difference between Ad4BP and ELP, and their distributions in steroidogenic tissues. Mol Endocrinol 8:643–653.

Mukai T, Kusaka M, Kawabe K, Goto K, Nawata H, Fujieda K, Morohashi K. 2002. Sexually dimorphic expression of Dax-1 in the adrenal cortex. Genes Cells 7:717–729.

Nagy A, Gertsenstein M, Vintersten K, Behringer R. 2003. Manipulating the mouse embryo: A laboratory manual, 3rd edition. New York: Cold Spring Harbor Laboratory Press.

Nakae J, Biggs WH III, Kitamura T, Cavenee WK, Wright CV, Arden KC, Accili D. 2002. Regulation of insulin action and pancreatic beta-cell function by mutated alleles of the gene encoding forkhead transcription factor Foxo1. Nat Genet 32:245–253.

Ogg S, Paradis S, Gottlieb S, Patterson GI, Lee L, Tissenbaum HA, Ruvkun G. 1997. The Fork head transcription factor DAF-16 transduces insulin-like metabolic and longevity signals in C. elegans. Nature 389:994–999.

Parry P, Wei Y, Evans G. 1994. Cloning and characterization of the t(X;11) breakpoint from a leukemic cell line identify a new member of the forkhead gene family. Genes Chromosomes Cancer 11:79–84.

Pierrou S, Hellqvist M, Samuelsson L, Enerback S, Carlsson P. 1994. Cloning and characterization of seven human forkhead proteins: Binding site specificity and DNA bending. EMBO J 13:5002–5012.

Renfree MB, Harry JL, Shaw G. 1995. The marsupial male: A role model for sexual development. Philos Trans R Soc Lond B Biol Sci 350:243–251.

Rossini GP, Pinna C, Viviani R. 1997. Inhibitors of phosphoprotein phosphatases 1 and 2A cause activation of a 53 kDa protein kinase accompanying the apoptotic response of breast cancer cells. FEBS Lett 410:347–350.

Semina EV, Brownell I, Mintz-Hittner HA, Murray JC, Jamrich M. 2001. Mutations in the human forkhead transcription factor FOXE3 associated with anterior segment ocular dysgenesis and cataracts. Hum Mol Genet 10:231–236.

Sinclair AH, Berta P, Palmer MS, Hawkins JR, Griffiths BL, Smith MJ, Foster JW, Frischauf AM, Lovell-Badge R, Goodfellow PN. 1990. A gene from the human sex-determining region encodes a protein with homology to a conserved DNA-binding motif. Nature 346:240–244.

Sorensen PH, Lynch JC, Qualman SJ, Tirabosco R, Lim JF, Maurer HM, Bridge JA, Crist WM, Triche TJ, Barr FG. 2002. PAX3-FKHR and PAX7-FKHR gene fusions are prognostic indicators in alveolar rhabdomyosarcoma: A report from the children's oncology group. J Clin Oncol 20:2672–2679.

Suri C, Jones PF, Patan S, Bartunkova S, Maisonpierre PC, Davis S, Sato TN, Yancopoulos GD. 1996. Requisite role of angiopoietin-1, a ligand for the TIE2 receptor, during embryonic angiogenesis. Cell 87:1171–1180.

Teh MT, Wong ST, Neill GW, Ghali LR, Philpott MP, Quinn AG. 2002. FOXM1 is a downstream target of Gli1 in basal cell carcinomas. Cancer Res 62:4773–4780.

Tilmann C, Capel B. 1999. Mesonephric cell migration induces testis cord formation and Sertoli cell differentiation in the mammalian gonad. Development 126:2883–2890.

Winnier GE, Hargett L, Hogan BL. 1997. The winged helix transcription factor MFH1 is required for proliferation and patterning of paraxial mesoderm in the mouse embryo. Genes Dev 11:926–940.

Zubair M, Ishihara S, Oka S, Okumura K, Morohashi K. 2006. Two-step regulation of Ad4BP/SF-1 gene transcription during fetal adrenal development: Initiation by a Hox-Pbx1-Prep1 complex and maintenance via autoregulation by Ad4BP/SF-1. Mol Cell Biol 26:4111–4121.

JHC ex*PRESS*
Accepted for publication on April 23, 2008
This article may be cited as DOI: 10.1369/jhc.2008.950543

Running Headline:

LOCALIZATION OF LOX-1 IN MURINE AND HUMAN PLACENTAS

JHC ex*PRESS*
Accepted for publication on April 23, 2008
This article may be cited as DOI: 10.1369/jhc.2008.950543

# Expression and Localization of Lectin-like Oxidized Low-Density Lipoprotein Receptor-1 (LOX-1) in Murine and Human Placentas

Hiroo Satoh, Emi Kiyota, Yasuhiro Terasaki, Tatsuya Sawamura, Katsumasa Takagi, Hiroshi Mizuta, Motohiro Takeya

Department of Cell Pathology (HS, EK, YT, MT), Department of Orthopaedic and Neuro-Musculoskeletal Surgery (HS, KT, HM), Graduate School of Medical and Pharmaceutical Sciences, Kumamoto University, Kumamoto, Japan

Department of Vascular Physiology (TS), National Cardiovascular Center Research Institute, Osaka, Japan

Correspondence to: Motohiro Takeya, Department of Cell Pathology, Graduate School of Medical Sciences, Kumamoto University, 1-1-1 Honjo, Kumamoto 860-8556, Japan.

Tel.: +81-96-373-5092; fax: +81-96-373-5096.

E-mail address: takeya@kumamoto-u.ac.jp.

Received for publication December 15, 2007; accepted April 23, 2008 [DOI: 10.1369/jhc.2008.950543].

JHC ex*PRESS*
Accepted for publication on April 23, 2008
This article may be cited as DOI: 10.1369/jhc.2008.950543

Abstract

Lectin-like oxidized low-density lipoprotein receptor-1 (LOX-1) is one of the scavenger receptors that recognizes oxidized low-density lipoprotein as a major ligand. The placenta is a major source of prooxidant during pregnancy, and the level of placental oxidative stress increases rapidly at the end of the first trimester and tapers off later in gestation. In our study, we evaluated placental expression of LOX-1 during different gestational stages in the mouse and human. We used immunohistochemistry and in situ hybridization to identify LOX-1-expressing cells in murine and human placentas. In both species, higher expression of LOX-1 mRNA during early to midgestational stages compared with late gestation —corresponding to the increased oxidative stress in early pregnancy— was revealed by real-time reverse transcription-polymerase chain reaction. In murine placenta, we demonstrated that LOX-1-expressing cells were fibroblast-like stromal cells in metrial glands and decidua basalis and that they were glycogen trophoblast cells in the junctional and labyrinth zones. In the human, LOX-1 expression was detected in villous cytotrophoblasts in both of first trimester and term placentas. These localization patterns of LOX-1 in murine and human placentas suggest the possible involvement of LOX-1 in high oxidative stress conditions of pregnancy.

Keywords: LOX-1, placenta, glycogen trophoblast cells, fibroblast-like stromal cells

Accepted for publication on April 23, 2008
This article may be cited as DOI: 10.1369/jhc.2008.950543

Introduction

Placental oxidative stress has been implicated in the pathogenesis of pregnancy-related complications such as miscarriage, preterm delivery, and preeclampsia (Hubel 1999; Burton and Jauniaux 2004). Highly reactive products of lipid peroxidation are formed when free radicals attack polyunsaturated fatty acids or cholesterol in lipoproteins. Oxidized low-density lipoprotein (ox-LDL) is a major product of lipid peroxidation. Elevated levels of antibodies to ox-LDL in women with established preeclampsia and in pregnant women with a history of repeated abortion indicate that uncontrolled lipid peroxidation and impaired ox-LDL elimination may induce cellular dysfunction and damage in the placenta (Branch et al. 1994; Tulppala and Ailus 1995). In isolated normal trophoblasts and placental macrophages, cellular uptake and degradation of modified LDL (scavenger receptor activity) were 20-fold higher than those of LDL (Bonet et al. 1995). Such scavenger receptor activity in the placenta may function to degrade modified lipoproteins and prevent toxic effects on placental cellular function and fetal growth and development (Bonet et al. 1995).

Lectin-like ox-LDL receptor-1 (LOX-1) is one of the scavenger receptors that is mainly expressed in vascular endothelial cells (Sawamura et al. 1997). It was initially cloned from bovine aortic endothelial cells and from human lung as a novel receptor for ox-LDL (Sawamura et al. 1997). LOX-1 shows strong activity for binding, internalizing, and degrading ox-LDL (Moriwaki et al. 1998). It is induced by stimuli including angiotensin II (Li et al. 1999), tumor necrosis factor-a (Kume et al. 1998), and advanced glycation end products (Chen et al. 2001) as well as ox-LDL itself (Aoyama et al. 1999). LOX-1 is involved in ox-LDL-induced apoptosis of vascular endothelial cells via intracellular production of reactive oxygen species (Li and Mehta 2000).

Accepted for publication on April 23, 2008
This article may be cited as DOI: 10.1369/jhc.2008.950543

LOX-1 is expressed not only in vascular endothelial cells but also in monocyte-derived macrophages, vascular smooth muscle cells, and chondrocytes (Yoshida et al. 1998; Moriwaki et al. 1998; Draude et al. 1999; Aoyama et al. 2000, Nakagawa et al. 2002). Northern blot analysis of human tissues detected LOX-1 mRNA in vascular-rich organs such as placenta, lung, brain, and liver (Sawamura et al. 1997). Among these tissues, the placenta had the highest expression of LOX-1 mRNA (Sawamura et al. 1997), which indicated the crucial role of LOX-1 in placental function. It is suggested that LOX-1 might be involved in trophoblast invasion in early pregnancy (Pavan et al. 2004; Fournier et al. 2007) and accelerated trophoblast apoptosis in preeclampsia (Lee et al. 2005). Immunohistochemical studies of human placenta showed that LOX-1 localized in extravillous trophoblasts of first trimester placenta (Pavan et al. 2004; Fournier et al. 2007) and in syncytiotrophoblasts of normal and preeclamptic term placentas (Lee et al. 2005). However, localization of LOX-1 in animals, especially the mouse—the best-studied mammalian experimental model system—has not been reported. In the present study, we describe the clear localization of LOX-1 in murine placenta, as determined by using immunohistochemistry and in situ hybridization, and we compared these results with data for human placenta.

## Materials and methods

### Sample collection

C57BL/6 mice were purchased from Japan Crea (Tokyo, Japan). Mice were bred in the Animal Resource Facility at Kumamoto University under specific-pathogen-free conditions. All animal procedures were approved by the Animal Research Committee at Kumamoto University, and all procedures conformed to Regulations for animal experiments of Kumamoto University. Adult female mice (2-5 months old) were mated with males in the evening and were monitored, starting the next morning, for the appearance of a vaginal plug. Noon on the day in which a vaginal plug was found was said to be 0.5 embryonic day (E0.5). Placentas were isolated at various developmental stages between days E10.5 and E18.5. For better tissue orientation, endometrial and myometrial components were not dissected away from placental disks during dissection. For investigation of the adult tissue distribution of LOX-1 mRNA, tissues were obtained from 8-week-old male mice.

Human placental tissues at 6-41 weeks of gestation were obtained from healthy pregnant women. Before collecting any such samples, we obtained signed informed consent, with consent documents written according to the Declaration of Helsinki, from all pregnant women in this study. First trimester placentas (6-12 weeks of gestation) and term placentas (37-41 weeks of gestation) were obtained from legal elective abortions and spontaneous vaginal deliveries, respectively.

### Reverse transcription-polymerase chain reaction (RT-PCR)

RNA isolation and RT were performed as previously described (Kobayashi et al. 2007). A

Accepted for publication on April 23, 2008
This article may be cited as DOI: 10.1369/jhc.2008.950543

1-mg sample of total RNA was used to produce cDNA with an Omniscript RT Kit (Qiagen, Valencia, CA, USA). The sequences of PCR primers used were as follows: mouse LOX-1 (522-bp product): forward primer: 5′-GAGCTGCAAACTTTTCAGG-3′, reverse primer: 5′-GTCTTTCATGCAGCAACAG-3′; human LOX-1 (193-bp product): forward primer: 5′-TTACTCTCCATGGTGGTGCC-3′, reverse primer: 5′-AGCTTCTTCTGCTTGTTGCC-3′; and glyceraldehyde-3-phosphate dehydrogenase (GAPDH) (392-bp product): forward primer: 5′-GGAAAGCTGTGGCGTTGGCGTGAT-3′, reverse primer: 5′-CTGTTGCTGTAGCCGTATTC-3′. These PCR primers were custom-made by Invitrogen (Carlsbad, CA, USA). The primers for GAPDH were designed to be available for both mouse and human.

The PCR cycle parameters were as follows: 15 min at 95 °C, three-step cycling (denaturation at 94 °C for 30 s; annealing at 55 to 60 °C for 30 s; and extension at 72 °C for 1 min), and 10 min at 72 °C using an iCycler™ Thermal Cycler (Bio-Rad Laboratories, Hercules, CA, USA). Thirty cycles were used for LOX-1; 28, for GAPDH . Annealing temperatures for LOX-1 and GAPDH were 55 °C and 60 °C, respectively. A 10-ml aliquot of each PCR product was then subjected to electrophoresis on 2% (w/v) agarose gel containing 0.1 mg/ml ethidium bromide.

Real-time PCR analysis

To quantify LOX-1 mRNA levels in murine and human placental tissues, real-time PCR was performed with an ABI PRISM®7700 Sequence Detection System (Applied Biosystems, Foster City, CA) as described earlier (Tsujita et al. 2007). A standard curve was constructed by plotting the relative amounts of a serial dilution of placental cDNA. Mouse placentas were

taken from at least 3 animals at each gestational age of E10.5, E11.5, E13.5, E14.5, E15.5, E16.5, E17.5 and E18.5. For human samples, first trimester placentas (6-12 weeks of gestation, n = 8) and term placentas (37-41 weeks of gestation, n = 5) were compared. For measurements, villi were separated from decidua and other components of first trimester placenta by using stereoscopic microscopy. Chorionic villi of central cotyledons were collected from term placentas. All experiments were performed in duplicate. Thermal cycler conditions consisted of 2 min at 50 °C (with uracil N-glycosylase for prevention of carryover contamination) and 10 min at 95 °C (for hot start PCR), followed by 40 cycles of 15 s at 95 °C and 1 min at 60 °C. Quantitative values of expression of target genes were determined as relative to endogenous 18S rRNA gene expression.

In situ hybridization

cRNA probes for mouse and human LOX-1 were synthesized from PCR-generated cDNA as described previously (Divjak et al. 2002) with minor modifications. PCR amplification of template PCR-generated cDNA (2.5 ml) was performed by using PrimeSTAR™ HS DNA Polymerase (Takara, Kyoto, Japan) with the following primer pairs: T7 mouse LOX-1 primer (544-bp product), 5′-CTTAATACGACTCACTATAGGGGAGCTGCAAACTTTTCAGG-3′ (forward primer) and 5′-CTTAATACGACTCACTATAGGGACAGATGTCAAGGCCAACA-3′(reverse primer); T7 human primer (544-bp product), 5′-CTTAATACGACTCACTATAGGGCTGGAGGGACAGATCTCAGC-3′ (forward primer) and 5′-CTTAATACGACTCACTATAGGGTTTCCGCATAAACAGCTCCT-3′ (reverse primer). PCR products were purified by using a High Pure PCR Product Purification

Kit (Roche Diagnostics, Mannheim, Germany). Next, purified PCR products were transcribed in vitro by means of T7 RNA polymerase and were labeled with digoxigenin (DIG)-dCTP via a DIG In Vitro Transcription Kit (Roche Diagnostics) to produce sense and antisense cRNA probes. Finally, cRNA probes were purified using a mini Quick Spin RNA column (Roche Diagnostics). Purified cRNA probes were mixed with equal volumes of deionized formamide (Wako, Osaka, Japan).

Murine and human placentas were fixed in 4% paraformaldehyde solution at 4 °C overnight and were then embedded in paraffin. Paraffin sections (3 mm) were deparaffinized in xylene and rehydrated in graded alcohols. Sections were treated with 10 mg/ml proteinase K (Roche Diagnostics) for 10 min at 37 °C and were postfixed in 4% paraformaldehyde, treated with 0.1 N HCl, and acetylated with 0.25% acetic anhydride in 0.1 mol/l triethanolamine (pH 8.0) for 10 min. Sections were then dehydrated in graded alcohols and air dried. Samples (50 ng) of cRNA probes were mixed with a 50-fold volume of hybridization buffer containing 50% formamide, 10 mM Tris-HCl (pH 7.5), 200 mg/ml tRNA, 1 × Denhardt's solution, 600 mM NaCl, 0.25% SDS, 1 mM EDTA (pH 8.0), and 10% dextran sulfate. The hybridization mixture was heat denatured, applied to dried sections, and covered with Parafilm. Hybridization was performed at 50 °C for 18 h in a humidified chamber. After hybridization, Parafilm was removed by a brief washing in 5 × SSC (1 × SSC: 150 mM NaCl plus 15 mM sodium citrate). Sections were then washed in 50% formamide plus 2 × SSC for 30 min at 50 °C. After the sections were washed in TNE (10 mM Tris-HCl pH 7.5, 0.5 M NaCl, 0.5 mM EDTA) for 10 min at 37 °C, they were treated with 10 mg/ml RNase A (Roche Diagnostics) for 30 min at 37 °C. They were again washed in TNE for 10 min at 37 °C and were then stringently washed sequentially, once in 2 × SSC and twice in 0.2 × SSC for 20 min at 50 °C. Sections were

washed in buffer 1 (100 mM Tris-HCl pH 7.5, 150 mM NaCl) for 5 min, were incubated with 1.5% blocking reagent (Roche Diagnostics) diluted in buffer 1, and were incubated for 30 min at room temperature (RT) with alkaline phosphatase-conjugated rabbit anti-DIG F(ab') fragment antibody (Roche Diagnostics) diluted 1:500 in buffer 1. After sections were washed twice in buffer 1 for 15 min and once in buffer 2 (100 mM Tris-HCl pH 9.5, 100 mM NaCl, 50 mM MgCl2) for 5 min, they were covered with 200 ml of buffer 2 containing nitroblue tetrazolium and 5-bromo-4-chloro-2-indolyl phosphate (Roche Diagnostics) and were placed in humidified chambers. Color development was monitored via a light microscope. Dark blue indicated a positive reaction. After a brief washing in tap water, sections were mounted in permanent aqueous medium (Nichirei, Tokyo, Japan). Counterstaining was not performed. Sections incubated with the sense probe served as negative controls.

Histology and immunohistochemistry

Formalin-fixed paraffin sections were stained with hematoxylin and eosin. Paraffin sections 3 mm thick were used to localize mouse desmin. Endogenous peroxidase activity in murine placental sections was blocked with 0.3% H2O2 in 100% methanol for 30 min at RT, after which sections were incubated for 90 min at RT with anti-human desmin rabbit polyclonal antibody (1 mg/ml, RB-9014-P; Lab Vision Ltd., Suffolk, UK), which cross-reacts with mouse desmin. An incubation for 30 min at RT with goat anti-rabbit Ig-conjugated peroxidase-labeled polymer amino acid (Nichirei) followed. Peroxidase activity was visualized by using 3,3′-diaminobenzidine tetrahydrochloride (Dojin Chemicals, Kumamoto, Japan) as the substrate. Meyer's hematoxylin was used as the counterstain. As a negative control, normal rabbit IgG (10 mg/ml; Santa Cruz Biotechnology, Santa Cruz, CA, USA) was

Accepted for publication on April 23, 2008
This article may be cited as DOI: 10.1369/jhc.2008.950543

used instead of the primary antibody.

For immunohistochemical studies of LOX-1, murine and human placental tissues were fixed with freshly prepared periodate-lysine-paraformaldehyde (PLP) fixative for 6-8 hours at 4 °C, after which they were washed with a graded series (10-20%) of sucrose in 0.1 M PBS. Fixed tissues were embedded in tissue-embedding media, frozen in liquid nitrogen, and cut into 6-mm-thick sections. Endogenous peroxidase activity in the murine placental sections was blocked as described above, followed by incubation of the sections for 90 min at RT with anti-mouse LOX-1 rat monoclonal antibody (JTX-58, rat IgG, 5mg/ml). Sections were then incubated for 30 min at RT with goat anti-rat Ig-conjugated peroxidase-labeled polymer amino acid (Nichirei). Visualization of peroxidase activity and counterstaining were performed as just described. As a negative control, normal rat IgG (10 mg/ml; Santa Cruz Biotechnology) was used instead of the primary antibody.

To stain human LOX-1, frozen sections of human placental tissues were incubated for 90 min at RT with biotinylated anti-human LOX-1 mouse monoclonal antibody (JTX-92, mouse IgG, 6.9 mg/ml). Sections were then incubated for 30 min at RT with avidin-biotin complex (VECTASTAIN® Elite ABC kit, Vector Laboratories, Inc., Burlingame, CA, USA). Peroxidase activity was visualized as described above. As a negative control, biotin-conjugated normal mouse IgG (10 mg/ml; Santa Cruz Biotechnology) was used instead of the primary antibody.

Electron microscopy and immunoelectron microscopy

Electron microscopic observation was performed as described previously (Komohara et al. 2005). For immunoelectron microscopy, frozen sections of PLP-fixed murine placentas were

Accepted for publication on April 23, 2008
This article may be cited as DOI: 10.1369/jhc.2008.950543

incubated overnight at 4 °C with anti-mouse LOX-1 monoclonal antibody (JTX-58). The sections were washed with PBS, after which they were incubated for 2 h at 4 °C with peroxidase-conjugated anti-mouse IgG [(F(ab')2] (Amersham, Buckinghamshire, UK). Peroxidase activity was visualized in the same way as noted above. Then samples were processed as previously described (Komohara et al. 2005). Ultrathin sections were evaluated via a Hitachi H-7500 electron microscope (Hitachi, Tokyo, Japan) without counterstaining.

Accepted for publication on April 23, 2008
This article may be cited as DOI: 10.1369/jhc.2008.950543

## Results

### Expression of LOX-1 mRNA in murine organs

By using RT-PCR, we examined the expression of LOX-1 mRNA in various organs of the mouse (Fig. 1A). The placenta had the highest level of LOX-1 mRNA expression. Lung and aorta showed moderate expression, and expression in other organs was weak or absent. To compare the level of LOX-1 mRNA expression in the placenta at various developmental stages, placental tissues from E10.5 to E18.5 were examined by means of real-time RT-PCR. Expression of LOX-1 mRNA peaked at midgestation (E14.5 to E15.5) and decreased thereafter (Fig. 1B).

### Compartment-specific expression of LOX-1 mRNA in murine placenta

Because strong LOX-1 mRNA expression was observed during midgestational days, placental tissue at E14.5 was used to examine the localization of LOX-1 protein and mRNA. The fundamental morphology of murine placenta is completed by midgestation, with the tissue being compartmentalized into four distinct regions: metrial glands (MG), decidua basalis (DB), junctional zone (JZ), and labyrinth zone (LZ) (Georgiades et al. 2002). The MG and DB belong to the maternal side, whereas the LZ and JZ belong to the fetal side. To examine the compartment-specific expression of LOX-1 mRNA, we separated pregnant uterus and placenta at E14.5 into four parts: myometrium, MG + DB, JZ + LZ, and yolk sac + amnion. RT-PCR analysis revealed stronger expression of LOX-1 mRNA in the MG + DB and LZ + JZ compared with the other two parts (Fig. 2).

### Localization of LOX-1 protein and mRNA in different compartments of murine placenta

At E14.5, the four compartments of the murine placenta have distinct histological features (Fig. 3A). To clarify the precise localization of LOX-1 expression in each compartment, we utilized immunohistochemistry and in situ hybridization. In agreement with results of RT-PCR analysis, LOX-1 protein was detected in these compartments, with distinct localization patterns. Diffuse LOX-1 staining was observed in the MG and the outer part of the DB (Fig. 3B). Strong cord-like staining in the JZ and faint diffuse staining in the LZ were also seen (Fig. 3B). No positive staining was observed in a negative-control section (Fig. 3C). In situ hybridization demonstrated clear co-localization of mRNA with the protein in all compartments (Fig. 3D). An in situ hybridization control section, with the sense probe, showed no positive signal (Fig. 3E).

Cellular localization of LOX-1 protein and mRNA in different compartments of murine placenta

In the mouse MG at midgestation, the major cellular components are granulated metrial gland (GMG) cells, also known as uterine natural killer (NK) cells, and fibroblast-like stromal cells. These two cell types are closely associated, with the fibroblast-like cells surrounding large, plump GMG cells (Fig. 4A). In immunohistochemical studies, LOX-1 was localized in the fibroblast-like cells but not in GMG cells (Fig. 4B). In situ hybridization clearly differentiated these two cell types: LOX-1 mRNA was detected in the cytoplasm of the fibroblast-like stromal cells surrounding the GMG cells (Fig. 4C). The expression pattern of LOX-1 mRNA in the fibroblast-like cells was in agreement well with that of desmin protein, a marker for this type of cell (Fig. 4D). Ultrastructural observation confirmed the intimate association of the fibroblast-like cells and the GMG cells (Fig. 4E). Immunoelectron